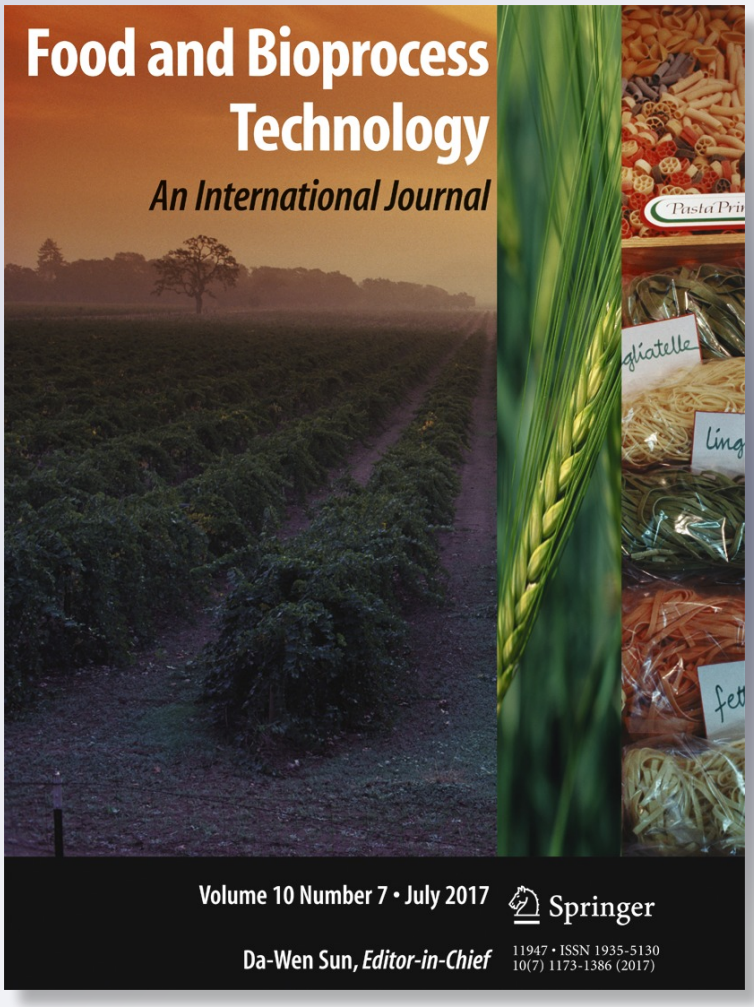
A Study on Structure (Micro, Ultra, Nano), Mechanical, and Color Changes of Solanum lycopersicum *L. (Cherry Tomato) Fruits Induced by Hydrogen Peroxide and Ultrasound*

Joaquín Fava, Andrea Nieto, Karina Hodara, Stella Maris Alzamora & María Agueda Castro

Food and Bioprocess Technology
An International Journal

ISSN 1935-5130
Volume 10
Number 7

Food Bioprocess Technol (2017)
10:1324-1336
DOI 10.1007/s11947-017-1905-4



Springer

Your article is protected by copyright and all rights are held exclusively by Springer Science +Business Media New York. This e-offprint is for personal use only and shall not be self-archived in electronic repositories. If you wish to self-archive your article, please use the accepted manuscript version for posting on your own website. You may further deposit the accepted manuscript version in any repository, provided it is only made publicly available 12 months after official publication or later and provided acknowledgement is given to the original source of publication and a link is inserted to the published article on Springer's website. The link must be accompanied by the following text: "The final publication is available at link.springer.com".



Author's personal copy

Food Bioprocess Technol (2017) 10:1324–1336
DOI 10.1007/s11947-017-1905-4

ORIGINAL PAPER

A Study on Structure (Micro, Ultra, Nano), Mechanical, and Color Changes of *Solanum lycopersicum* L. (Cherry Tomato) Fruits Induced by Hydrogen Peroxide and Ultrasound

Joaquín Fava[1] · **Andrea Nieto**[2,3] · **Karina Hodara**[4] · **Stella Maris Alzamora**[2,3] · **María Agueda Castro**[5]

Received: 6 July 2016 / Accepted: 14 March 2017 / Published online: 29 March 2017
© Springer Science+Business Media New York 2017

Abstract Changes in the epidermis structure (micro, ultra, and nano), mechanical properties, and surface color of *Solanum licopersicum* L. fruits (cherry tomatoes) due to hydrogen peroxide (HP) and high-power ultrasound (US) treatments were examined. Both treatments induced small alterations in the epicuticular waxes, the cuticular membrane, and the epidermal and subepidermal cells. Plasmolysis of subepidermal cells, slight epicarp compression, and dense cellulose microfibrils pattern in the non cutinized cellulose layer were documented after US. Looser cellulose microfibrils pattern in the cutinized and non cutinized cellulose layer was detected after HP exposure. Main nanostructure alterations in the cellulose domain affected the morphology and size of cellulose aggregates and nanofractures of cellulose layer in treated fruits. US treatment decreased a^*, b^*, and chroma values by 10, 5, and 7% and increased L^* and hue angle by 2.5 and 3%, respectively, as compared to raw fruits. These small but significant differences were attributed to the disruption of the wax layer; color became brighter, more vivid, and more orange. Treatments slightly affected puncture parameters; the rupture force decreased from 14.8 N to 14.1 N and 13.8 N; the penetration probe at the rupture point increased from 7.6 mm to 7.7 mm and 8.0 mm and the mechanical work decreased from 48.7 mJ to 48.3 mJ and 44.4 mJ in raw fruits and after HP and US exposure, respectively. The mechanical response could be partially explained by the alterations in the micro, ultra, and nanostructure of the tissues. The low impact of US and HP treatments on mechanical and color characteristics would indicate their potential for cherry tomatoes decontamination.

Keywords Cherry tomatoes · Epidermis structure · Mechanical properties · Color · Hydrogen peroxide · Ultrasound

✉ Stella Maris Alzamora
smalzamora@gmail.com

✉ María Agueda Castro
macastro681@gmail.com

[1] Grupo de trabajo sobre Conservación de la Biodiversidad, Subsecretaría de Planificación y Política Ambiental, Secretaría de Ambiente y Desarrollo Sustentable, San Martín 451, 1004 C.A.B.A., Argentina

[2] Departamento de Industrias, Facultad de Ciencias Exactas y Naturales, Universidad de Buenos Aires, Ciudad Universitaria, 1428 C.A.B.A., Argentina

[3] Consejo Nacional de Investigaciones Científicas y Técnicas de la República Argentina, Godoy Cruz 2290, 1425 C.A.B.A., Argentina

[4] Departamento de Métodos Cuantitativos y Sistemas de Información, Facultad de Agronomía, Universidad de Buenos Aires, Av. San Martín 4453, 1417 C.A.B.A., Argentina

[5] Anatomía Vegetal Aplicada, Departamento de Biodiversidad y Biología Experimental, Facultad de Ciencias Exactas y Naturales, Universidad de Buenos Aires, Ciudad Universitaria, 1428 C.A.B.A., Argentina

Introduction

The consumption of fresh and minimally processed fruits and vegetables has significantly increased over the few last decades associated not only with an evident concern about high quality but with their role for improving human well-being (Allende et al. 2006). In terms of conventional antioxidants, tomatoes provide an excellent amount of vitamin C and beta-carotene, a very good amount of the mineral manganese, and a good amount of vitamin E. In terms of phytonutrients, they have flavonones, flavonols, hydroxycinnamic acids, carotenoids (including their oftentimes-rich concentration of

Author's personal copy

lycopene), glycosides, fatty acid derivatives, and 9-oxo-octadecadienoic acid (George et al. 2004; Balasundram et al. 2006).

Intake of tomatoes has long been linked to heart health. They have been shown to help lower total cholesterol, LDL cholesterol, and triglycerides. In addition, they prevent aggregation of platelet cells in the blood, support bone health, provide us with anti-cancer benefits, and reduce risk of some neurological diseases (Rao and Agarwal 2000; Sharoni and Levi 2006; Wilcox et al. 2003; Martínez-Valverde et al. 2002).

Microorganisms are natural contaminants of fresh fruits and vegetables and come from different sources including post harvest handling. To reduce the microbial (pathogenic and spoilage) load on the produce surface, new decontamination strategies that do not result in toxic residues are being evaluated, among them washing with hydrogen peroxide solutions (HP) and application of high power ultrasound (US). Inactivation of microorganisms by high-power ultrasonic waves has been attributed to the cavitation phenomenon. Microbubbles of gas and/or vapor formed within a liquid during the rarefaction cycle of the acoustic wave undergo violent collapse during the compression cycle of the wave. This implosion or cavitation releases large amounts of energy, generating temperatures of several thousand Kelvin and shock waves with pressures of several atmospheres (Mason 1990). Hydrogen peroxide is effective against a wide spectrum of bacteria, yeast, molds, viruses, and spore-forming organisms. H_2O_2 has been shown to damage bacterial proteins, DNA, and cellular membranes of microbial cells and to remove protein from the coat of the bacterial spore (Juven and Pierson 1996). Its toxicity appears to be not due to its oxidative properties in its molecular state but to the formation of other more reactive oxidant species (hydroxyl radical, superoxide, and singlet oxygen) in oxygen and H_2O_2 reduction.

Sao José and Vanetti (2012) reported that US treatment (10 or 20 min, 45 kHz) lead to reductions up to 1.0 log CFU/g of aerobic mesophiles and 1.22 log CFU/g of *Salmonella Typhimurium* adhered on surface of whole cherry tomatoes, while 5% HP results in approximately 2.6 log CFU/g reduction in contamination at room temperature. Wang et al. (2015) demonstrated that US (800 W, 35 μm amplitude) of appropriate power density reduced the population of total bacteria and of mold and yeast by 0.86 and 0.70 log CFU/g, respectively, while maintaining flavor and nutritional quality of postharvest cherry tomatoes.

In a consumer study with cherry tomatoes carried out by Pagliarini et al. (2001), internal preference mapping revealed two consumer clusters: one that prefer red color and sweet taste and one that preferred acidity and firm texture. Thus, for consumer's perception of fruit quality, texture and color are critical attributes. The cherry type is a popular fresh tomato specialty having a small size and firm texture. Their skin acts as a hydrophobic barrier which protects the fruit from physiological and climatic injuries, dehydration, fungal infection, and UV-C light, and contributes to fruit firmness and shelf-life (Pinelo et al. 2006). Epidermal cells are organized in a continuous (without air spaces between cells) and uniform monolayer of strongly attached cells with an asymmetrical cell wall deposition (Domínguez et al. 2011). The outer cell wall is much thicker than the inner epidermal wall and can be distinguished from all other cell walls of plants by the presence of thick continuous lipidic layers deposited on its outermost region (Jeffree et al. 1976; Wattendorff and Holloway 1980). In general, five defined layers can be detected from outer to inner (Fig. 1): (1) epicuticular wax layer, ew (amorphous, crystalline or semi-crystalline); (2) cuticle proper, c (constituted only by cutin); (3) cutinized layer, cl (mainly composed by a polysaccharide matrix, cutin, and intracuticular waxes). Cuticle proper and cutinized layers constitute the cuticular membrane, CM (Esau 1977); (4) peptic layer, pl (mainly composed by pectic polysaccharides); and (5) non cutinized cellulose layer or cellulose layer, cw (Baker 1982; Holloway 1982), which is a strong network of cellulose microfibrils linked by hydrogen bonding to xyloglucans, pectic polysaccharides, and additional minor cell wall constituents (structural proteins, enzymatic proteins, hydrophobic compounds, and inorganic molecules) (Carpita and Gibeaut 1993; Cosgrove 2001). Next to epidermis, collenchyma tissue appears constituted by several (3–4) cell layers, which can also have wall thickenings that contribute to the mechanical support.

Ultrasound and hydrogen peroxide treatments could impact over the cherry tomato skin causing alterations and affecting

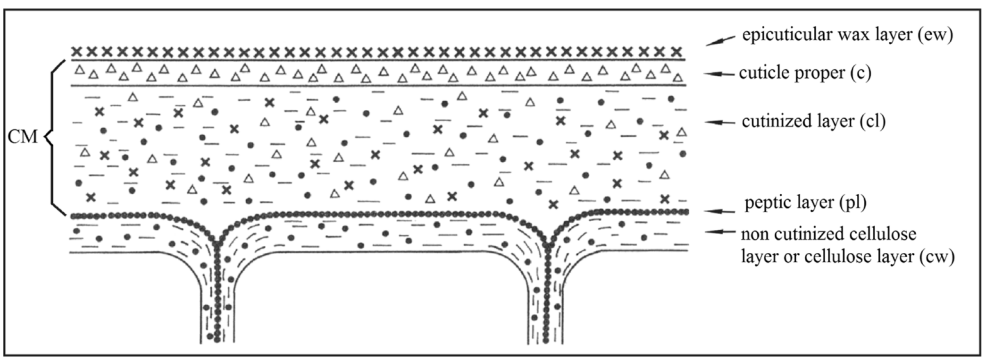


Fig. 1 Scheme showing the different layers of the outer wall of epidermal cells. *X mark* indicates wax, *empty triangle* indicates cutine, *filled circle* indicates pectins. and *dash* indicates cellulose; *CM* cuticular membrane

Author's personal copy

the appearance of the fruit, its resistance to cracking, and its ability to resist shipping and marketing. Little is known about structural effects of high-power ultrasound and hydrogen peroxide treatments as well as their impact on tomato cherry quality. The knowledge of structural epidermis changes due to treatments along with the integration of macroscopic mechanical and color analysis would help to identify the causes of texture and color changes and provide new insights to design successful preservation techniques.

The present study examined the structure alterations occurred mainly in the skin of *Lycopersicon esculentum* L. (cherry tomato) var. cerasiforme fruits after hydrogen peroxide and high-power ultrasound treatments using complementary microscopic techniques and their impact on color and mechanical properties.

Materials and Methods

Sample Preparation

Solanum lycopersicum L. (cherry tomato) var. cerasiforme Alef Supersweet 100 plants were cultivated in greenhouse (Faculty of Agronomy, C.A.B.A., Argentina). Cherry tomato fruits (spherical in shape, about 25 mm in diameter, red ripeness stage), without detaching the pedicel, were harvested at random. They were then divided in three sets of 45–50 fruits and placed in low density polyethylene bags maintained at 4–5 °C for a maximum period of time of 1 day before use.

Cherry tomato fruits with attached calyx and pedicels were subjected to different treatments: one group was exposed to hydrogen peroxide immersion and the second one to high-power ultrasound. Another group of raw fruits was selected as control. The treated and untreated groups were examined for structure, color, and mechanical properties immediately after treatments.

Hydrogen Peroxide Treatment

Treatment was carried out at 25 °C in a 900-mL glass flask with 600 mL of sterile citric acid-Na_2HPO_4 buffer solution (pH 3.0) containing 34.3 mL of hydrogen peroxide to obtain a final solution with 2.0% (*w*/*v*) concentration. The disinfectant agent solution was prepared from 35% (*w*/*v*) hydrogen peroxide solution (Merck, Darmstadt, Germany). The buffer solution was prepared from 0.1 M citric acid monohydrate (J.T. Baker, Phillipsburg, USA) and 0.2 M Na_2HPO_4 (M&B, Dagenham, England). H_2O_2 levels were monitored by titration with 0.1 N potassium permanganate (Mallinckrodt, Phillipsburg, USA) immediately before and after treatment. The pH was measured with a pH meter Mettler Toledo (model MP 220, Schwerzenbach, Switzerland).

Cherry tomatoes were immersed during 2 min in the sanitizing agent solution, and transferred into a bath with distilled water at 25 °C as neutralizing solution by 1 min.

Sanitizing treatment conditions (pH, hydrogen peroxide concentration, and immersion time) were selected due to their great effectiveness against microorganisms, according to previous studies by Raffellini et al. (2011).

Ultrasonic Treatment

Treatment was carried out in a 500-mL double wall cylindrical vessel (diameter 9.5 cm; height 14.5 cm) connected to a thermostatically controlled water bath (HAAKE, Model Rotovisco RV12, Germany) whose temperature was fixed to attain 40.0 ± 0.2 °C in the samples. Eight fruits were placed in a fixed stainless steel net into the vessel at 15 mm of distance from the tip, around the 13 mm ultrasound probe (tip size 12.7 mm), and 400 mL distilled water was added. The fruits were immediately sonicated.

Ultrasound (Vibracell®, net power output: 600 W, Sonic Materials Inc., Chicago) at 20 kHz and 95.2 (80%) μm of wave amplitude was applied to the cherry tomatoes during 5 min. Ultrasonic time longer than 5 min caused the rupture of the skin fruit. After 2 min of sonication, the desired temperature was reached and it was maintained constant throughout the experiment by recycling water 10 °C below the selected value. Due to bubbles generated by cavitation, the system was always highly mixed from the start of the experiment.

Previous studies have shown that the selected amplitude of ultrasonic process was the most suitable, since further increases in amplitude did not result in a greater microbial inactivation (Guerrero et al. 2001; López-Malo et al. 1999).

Microscopic Observations

Environmental scanning electron microscopy (ESEM), light microscopy (LM), transmission electron microscopy (TEM), and atomic force microscopy (AFM) were used to examine micro, ultra, and nanostructure in raw and in treated cherry tomatoes.

For ESEM, rectangular strips (15 mm length, 10 mm width) of epicarp were excised, mounted on metal supports and observed using an Electroscan 2010 (Wilmington, MA, USA) Environmental Scanning Electron Microscope operating at 10.0–20.0 kV and 267–667 Pa.

For LM study, transverse ultrathin sections (1 μm thick) were stained on slide with 0.05% (*w*/*v*) toluidine blue in 2.5% (*w*/*v*) Na_2CO_3 solution (pH 11.1) for 1–6 min at 60 °C, and examined under a Zeiss Phomi III Microscope (Oberkochen, Germany). All reactives were from Merck Química Argentina S.A. (Argentina).

For TEM, the outermost region of pericarp was excised in pieces of about 1 mm^3 with a scalpel and fixed in 3%

Author's personal copy

(*v*/*v*) glutaraldehyde in 0.2 M Na_2HPO_4 - Na_2HPO_4 buffer solution (pH 7.4) at 4 °C for 12 h. Samples were then washed with the buffer for 24 h and postfixed in 1% (*w*/*v*) OsO_4 aqueous solution at 20 °C for 2 h. Samples were washed with the same buffer for 1 h, dehydrated in an ascending ethanol series (50, 70, 90, 100% (*v*/*v*), 15 min each) and ethanol-acetone series (2:1, 2:2, 1:3; pure acetone, 15 min each) at 20 °C, and embedded in low viscosity Spurr' s resin (Spurr 1969). Ultrathin sections (1 μm thick) were cut using a glass knife with a Sorvall MT 2-B ultracut microtome, collected on copper grids and double stained with uranyl acetate and Reynolds lead-citrate (Reynolds 1963). Sections were examined using a JEOL JEM 1200 EX II Transmission Electron Microscope (Tokyo, Japan) at an accelerating voltage of 90 kV.

For AFM, ultrathin sections were cut using a glass knife with a Sorvall MT 2-B ultracut microtome, collected unstained on cover glasses, mounted on mica disks, and examined in a Multimode Atomic Force Microscope with a NanoScope III A-Quadrex controller III (Digital Instruments-Veeco, Santa Barbara, CA, USA). Topography, amplitude, and phase images were acquired simultaneously by using the tapping mode under dried N_2. The AFM tips (silicon cantilevers) were 125 μm long and had a nominal spring constant of 40 N/m (TAP 300, Nano Devices, Santa Bárbara, USA). The scan area sizes varied from 15 × 15 to 1 × 1 μm. The scan rate applied was 1–5 Hz.

Evaluation of Mechanical Properties

Puncture test on whole cherry tomatoes was performed using an Instron Universal Testing Machine model 1011 (Canton, MA, USA) with a stainless steel plunger with a flat end cylindrical probe (4 mm in diameter), at a deformation speed of 50 mm/min and a load range of 20 N at ambient temperature (25 ± 1 °C) and 85% of relative humidity. The force was recorded every 0.33 s. Each specimen was placed on a flat steel holder (10 mm thick) with a hole (10 mm in diameter) in the center and was penetrated on the equatorial side (perpendicular to the abscission zone). From the force-displacement curve, three mechanical parameters were computed. The maximal rupture force (F_R, expressed in N) represents the force required to puncture the cherry tomato skin. The probe position at F_R (D_R, expressed in mm) indicates the penetration depth of the probe from the first contact with the fruit to the point of rupture. The mechanical work (*W*, expressed in mJ) corresponds to the energy needed to break the skin and was estimated by the area under the curve up to the skin rupture point. Puncture measurements were performed immediately after treatments on 30 cherry tomato fruits from each group.

Color Measurement

Cherry tomato surface color was measured with a handheld tristimulus reflectance spectrocolorimeter Model CM-508-d (Minolta Co., Japan) by using a 1.4 cm measuring aperture and a white background. Values were obtained for *C* illuminant and 2° observer. Before the test, the instrument was calibrated with a standard black glass and a standard white provided by the manufacturer.

The C.I.E color coordinates (*X*, *Y*, *Z*) and the *L**, *a**, and *b** components of the CIELAB space were recorded, where *L** indicates lightness or luminance, *a** indicates chromaticity on a green (−) to red (+) axis, and *b** chromaticity on a blue (−) to yellow (+) axis. These numerical values were converted into "chroma" (*C*) and "hue angle" (*h*) color functions using the following equations:

$$C = \left(a^{*2} + \mathrm{b}^{*2}\right)^{1/2} \quad (1)$$

$$h = \mathrm{arctg}\left(b^*/\mathrm{i}^*\right) \quad (2)$$

Hue angle can be distributed in the four quadrants of the *a** *b** plane (red-purple 0°, yellow 90°, bluish-green 180°, and blue 270°) and chroma represents the intensity or purity of the hue.

Color was evaluated in raw cherry tomato (control) and in treated fruits immediately after processing. Ten independent samples were used for each condition with two readings taken at two different positions in the equatorial zone of each fruit. The reported results were based on the average value.

Statistical Analysis

Statistical analyses were carried out using InfoStat Versión 2009 (InfoStat Group, UNC, Córdoba, Argentina). Mechanical and color data were analyzed by multivariate analysis of variance (MANOVA) (Quinn and Keough 2002). Three and five response variables were taken from mechanical and color analysis, respectively. Post-hoc multiple comparisons among multivariate means of treatments were performed by Hotelling tests based on Bonferroni correction. Discriminant function analysis (DFA) was applied as an extension of multivariate analysis of variance (McGarigal et al. 2000). Previously to the analyses, the assumptions of homogeneity of variance-covariance matrices and multivariate normal distribution were tested. Multivariate outliers were detected by Mahalanobis distance and removed from data set. Multicolinearity among response variables was assessed by the Pearson correlation matrix, and only uncorrelated variables were entered into the MANOVA and DFA analyses. Values of $p < 0.05$ were considered to be significant in all analyses.

Author's personal copy

Results and Discussion

Microscopic Features

Raw Cherry Tomato

Raw cherry tomatoes, between 20 and 25 mm in diameter, were red colored, turgent, and rounded in shape. Epicarp exhibited intact and uniform general aspect, with a smooth and intense bright surface (Fig. 2a).

With ESEM and in superficial view, the epicarp of raw fruits showed polygonal epidermal cells with a depressed central area and a prominent perimeter elevated over the epidermis level. Epicuticular waxes constituted a smooth layer (Fig. 3a).

LM analysis of transverse sections showed the epicarp composed by one stratum of epidermis and three or four subepidermic collenchymatous layers. In general, epidermal cells exhibited quadrangular shape, parietal cytoplasm, turgent central vacuole, thick outer tangential walls, and thinner radial and inner walls. Throughout the inner tangential and radial cell walls, the cuticular membrane (i.e., cuticle proper and cutinized layers) appeared extended in variable degree, and constitutes conspicuous wedges between two consecutive epidermal cells. Mesocarp (edible pulp) presented evident intercellular spaces and rounded to irregular turgent cells with parietal cytoplasm (Fig. 4a).

TEM study showed the epicuticular waxes as a continuous, translucent thin stratum with a sinuous electron dense contour. Cuticle, about 2.5–3.5 μm thick, appeared well defined, amorphous, and with smooth contour. A gradual delimitation between cuticle and cutinized layer was observed (Fig. 5a). Cutinized layer, electron dense and about 2.5 μm thick, exhibited reticulated pattern. The layer of peptic polysaccharides marked an abrupt transition with non cutinized cellulose layer. Translucent non cutinized cellulose layer, about 2–3 μm thick, showed the framework of cellulose microfibrils. Between two consecutive epidermal cells and throughout the radial wall a conspicuous wedge of CM and peptic layer was observed (Fig. 5b). In general, epidermal cells presented parietal cytoplasm and central vacuole (Fig. 5b).

AFM observations (amplitude image types) taken at 30 × 30,15 × 15, and 5 × 5 μm areas showed a partial view of the outer tangential epidermal cell wall with a well-delimited transition between cuticle, cutinized layer, and non cutinized cellulose layer (Fig. 6a, b). The peptic layer was clearly observed between the cutinized and non cutinized layers. Amplitude image type (5 × 5 μm) of the cuticular membrane (outermost region) documented the cuticle nanoporosity (Fig. 6c). Topography and amplitude image type (1 × 1 μm areas) of the non cutinized cellulose layer showed the evident cellulose microfibril framework intermixed with several irregular nanopores, variables in size, and distributed without a defined pattern (Fig. 7a, b). Three-dimensional representation (1 × 1 μm area) documented the visible cellulose microfibril framework and nanopores (Fig. 7c).

Hydrogen Peroxide Treated Cherry Tomatoes

In superficial view, treated cherry tomatoes presented a general aspect similar to the control one, with uniform intact epicarp, and firm consistence (Fig. 2b).

ESEM superficial images evidenced polygonal epidermal cells with a markedly depressed central area and prominent perimeter somewhat similar to the control ones. However, the epicuticular wax layer looked altered and exhibited evident, numerous and irregular disruptions randomly distributed (Fig. 3b).

LM images of transverse sections revealed that the structure of cherry tomatoes undergone hydrogen peroxide treatment was similar to the control one, corroborating that the effect of the sanitizer was mainly at surface level (Fig. 4b).

TEM analysis showed the localized absence of epicuticular waxes (micrographs not shown). Wax layer disruptions appeared randomly distributed. When present, wax layer exhibited a slight thickness increase and undulate contour. Gradual transition between cuticle and cutinized layer was observed (Fig. 5d). Cuticle with smooth superficial contour was amorphous and well defined. The outer zone of the cutinized layer presented a loose reticulated pattern of polysaccharides; the electron dense inner zone exhibited a more packed pattern distribution of polysaccharides. Besides, an abrupt transition between cutinized layer and non cutinized cellulose layer was observed (Fig. 5c, d). Electron less dense non cutinized cellulose layer, about 3–3, 2 μm thick, exhibited cellulose microfibrils with a loose pattern distribution. The presence of parietal cytoplasm and vacuole evidenced the cytological integrity of epicarp cells (Fig. 5c).



Fig. 2 Pictures of *Solanum lycopersicum* L. var. cerasiforme. **a** Raw cherry tomatoes. **b** Hydrogen peroxide treated cherry tomatoes. **c** Ultrasound-treated cherry tomatoes. *Scales*, **a**–**c** is 2 cm

Author's personal copy

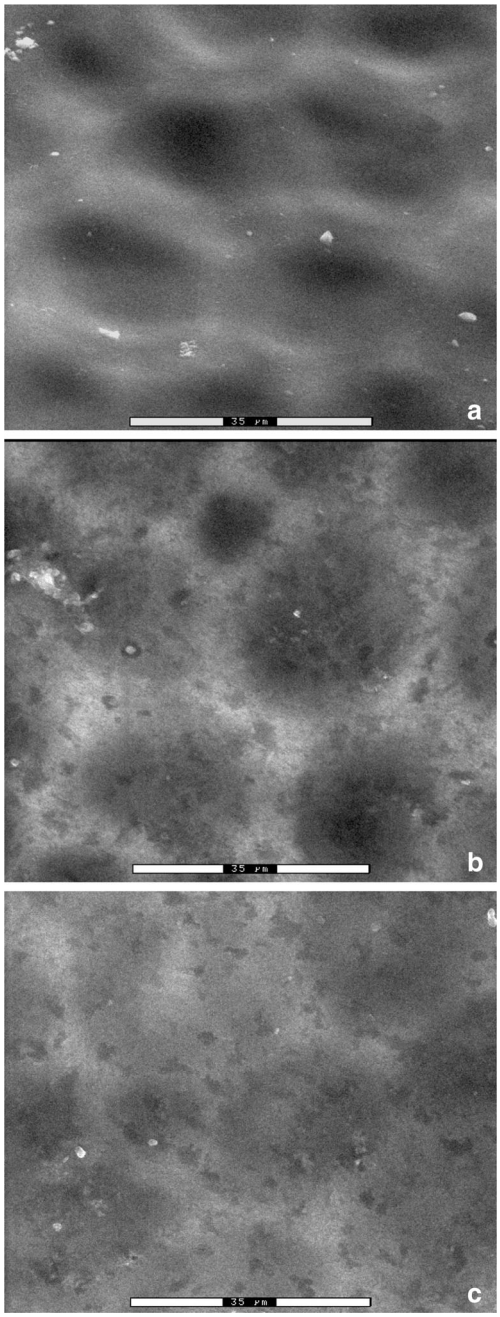


Fig. 3 *Solanum lycopersicum* L. var. cerasiforme ESEM micrographs, epicarp, (superficial views), general aspects and details. **a** Raw cherry tomatoes. **b** Hydrogen peroxide treated cherry tomatoes. **c** Ultrasound-treated cherry tomatoes. *Scale* is 35 μm

AFM observations (amplitude image types) taken at 15 × 15 and 2 × 2 μm areas revealed gradual transition between cuticle and cutinized layer and abrupt transition between cuticular membrane and non cutinized cellulose layer. In general, after treatment, the epicuticular wax layer showed undulate contour. Cuticle appeared more compact respect to the control one (Fig. 6d–e). The amplitude image types taken at 2 × 2 μm area documented the loose middle and innermost region of the cutinized cellulose layer, the radial pattern distribution of polysaccharides, and the presence of numerous and irregular nanopores (Fig. 6f). Topography and amplitude image types at 1 × 1 μm of non cutinized cellulose layer showed the framework of cellulose microfibrils altered respect to the control one. Conspicuous cellulose aggregates and nanopores were documented. Nanopores appeared narrow to elongate (Fig. 7d, e). Three-dimensional representation

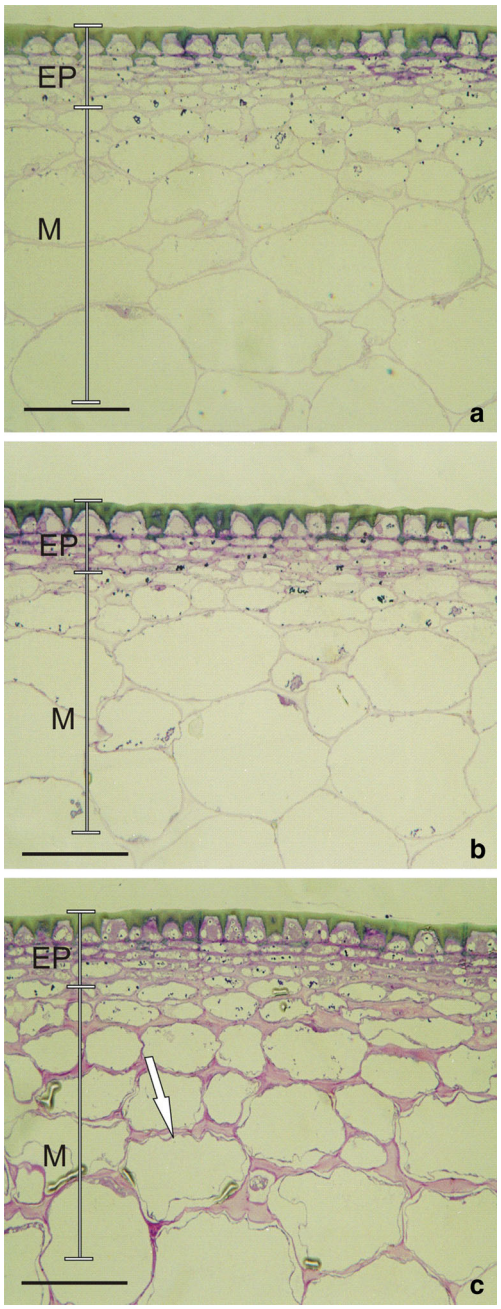


Fig. 4 *Solanum lycopersicum* L. var. cerasiforme LM micrographs, epicarp, and mesocarp (transverse sections). **a** Raw cherry tomatoes, epicarp and mesocarp, general aspect. **b** Hydrogen peroxide treated cherry tomatoes. **c** Ultrasound-treated cherry tomatoes. *EP* epicarp, *M* mesocarp; *white arrow* indicates plasmolysis. *Scales*, **a**–**c** is 100 μm

Author's personal copy

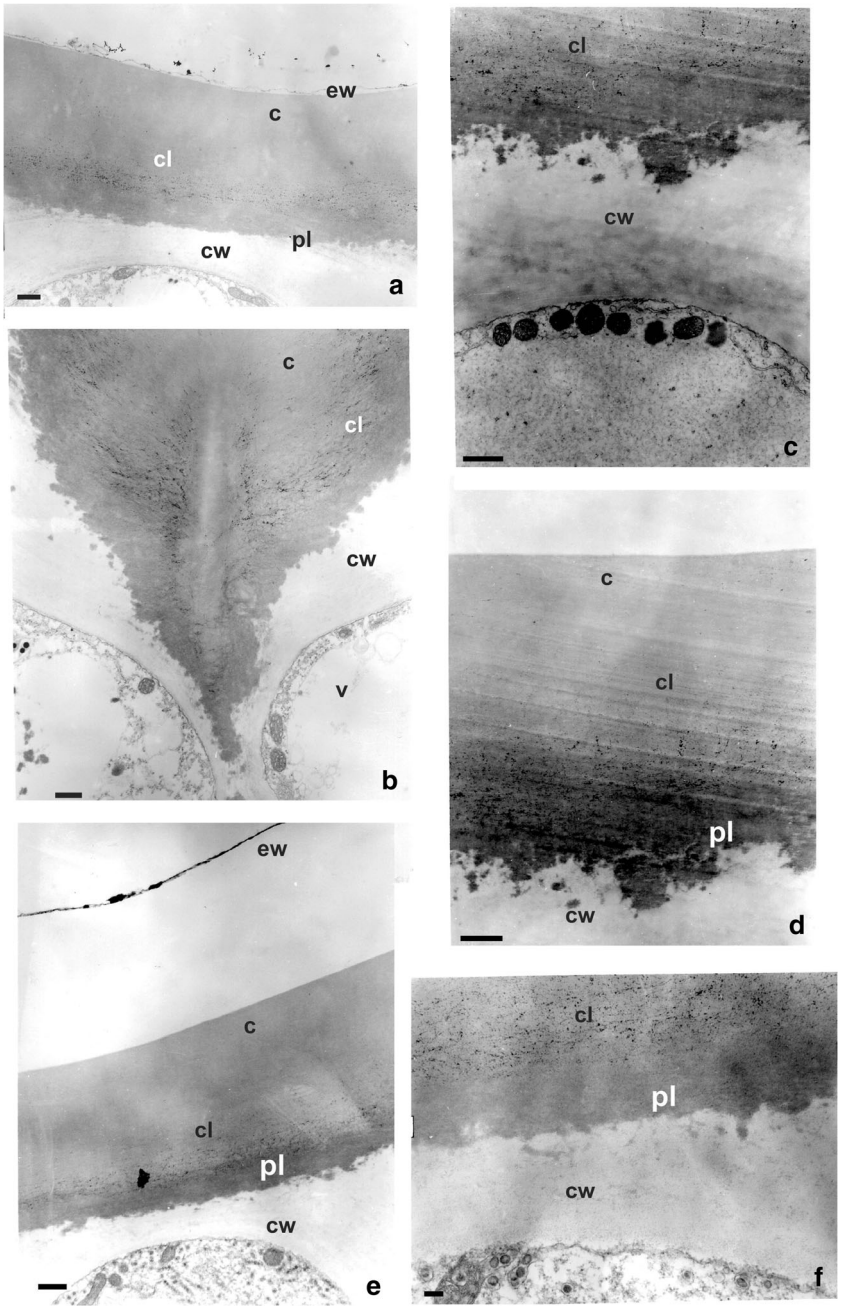


Fig. 5 *Solanum lycopersicum* L. var. cerasiforme TEM micrographs (transverse sections). **a**, **b** Raw cherry tomatoes. **a** Outer tangential epidermal cell wall, general spect. **b** Wedge of cuticular membrane between two consecutive epidermal cells. **c**, **d** Hydrogen peroxide treated cherry tomatoes. **e**, **f** Ultrasound-treated cherry tomatoes. *c* cuticle, *cl* cutinized layer, *cw* non cutinized cellulose layer, *ew* epicuticular wax layer, *pl* peptic layer, *v* vacuole. *Scales*, **a–e** is 1 μm, **f** is 500 nm

(1 × 1 μm area) exhibited the cellulose microfibrils pattern alteration (Fig. 7f).

Ultrasound-Treated Cherry Tomatoes

In superficial view, sonicated cherry tomatoes were rounded in shape, red in color, and with bright surface, somewhat less intense than the in control one. Epicarp was continuous, without evident disruptions. Occasional delimited areas appeared slightly depressed and with rough surface.

With ESEM, polygonal epidermal cells exhibited a rather prominent perimeter and depressed central area. Frequent and irregular disruptions of epicuticular wax layer were randomly distributed over the surface. The pattern of disruption produced by ultrasound was essentially the same as that noted in hydrogen peroxide exposed fruits but slightly more accentuated, suggesting changes in the conformation and distribution of epicuticular waxes (Fig. 3c).

LM observations of transverse sections showed quadrangular epidermal cells with dense cytoplasm and turgent vacuoles. Epicuticular wax layer appeared disrupted. When present, this layer was next to and/or separate from the cuticle. Subepidermic collenchymatous cells exhibited swollen walls. Somewhat compact mesocarp because of intercellular spaces

Author's personal copy

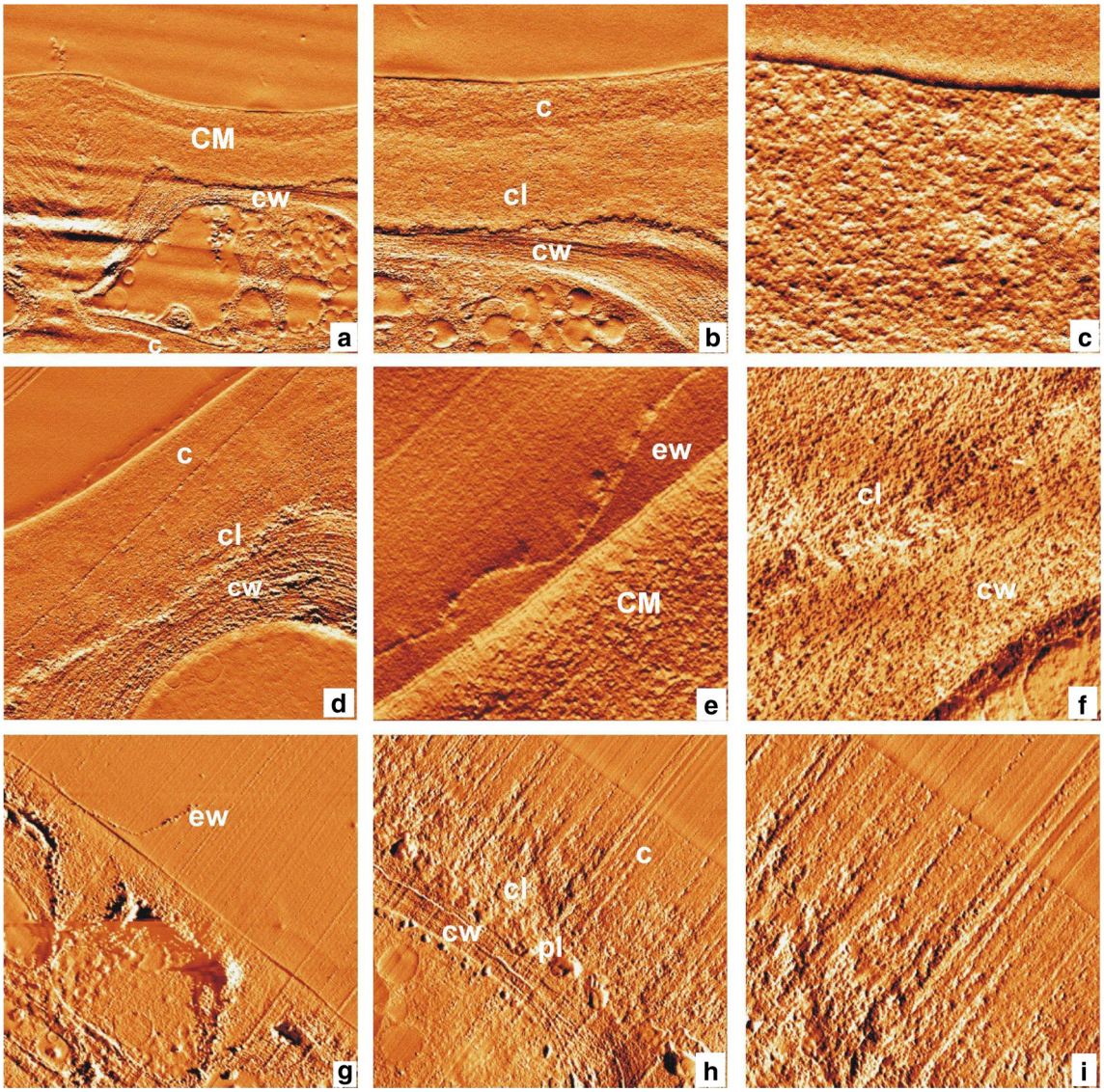


Fig. 6 *Solanum lycopersicum* L. var. cerasiforme AFM micrographs (amplitude image types). **a–c** Raw cherry tomatoes, outer tangential epidermal cell wall. **a** Epidermal cell partial view. **b** Outer tangential epidermal cell wall. **c** Smooth epicuticular wax layer, and cuticle. **d–f** Hydrogen peroxide treated cherry tomatoes. **d** Outer tangential epidermal cell wall, general aspect (amplitude image type). **e** Undulated epicuticular wax layer and partial view of the cuticular membrane (amplitude image type). **f** Cutinized layer and non cutinized cellulose layer, phase image type. **g–i** Ultrasound-treated cherry tomatoes, amplitude images types. **g** Epidermal cells and disrupt epicuticular wax layer. **h** Outer tangential epidermal cell wall. **i** Cuticle and non cutinized cellulose layers. *c* cuticle, *cl* cutinized layer, *pl* peptic layer, *cw* non cutinized cellulose layer, *ew* epicuticular wax layer. Scan sizes, **a** is 30 × 30 μm, **b** is 15 × 15 μm, **c–i** is 5 × 5 μm, **d** is 15 × 15 μm, **e–f** is 2 × 2 μm, **g** is 50 × 50 μm, **h** is 10 × 10 μm

reduction showed the parenchyma cells irregular in shape with undulated contour, incipient plasmolysis, and thick walls (Fig. 4c).

TEM study confirmed alteration of the epicuticular wax layer. In transverse sections, it appeared detached from the cuticle (Fig. 5e) or could not be visualized (micrographs not shown). Amorphous cuticle showed smooth superficial contour. CM and peptic layer appeared well delimited and with accentuated electron density. Non cutinized cellulose layer exhibited altered framework of cellulose microfibrils, rather electron dense (Fig. 5e, f).

AFM observations (amplitude image types) taken at 50 × 50, 10 × 10, and 5 × 5 μm area documented the detached and/or disrupted epicuticular wax layer (Fig. 6h, i). Occasionally, it appeared smooth and attached to the CM (Fig. 6g). Well-delimited transitions between cuticle, cutinized cellulose layer, and non cutinized cellulose layer were observed (Fig. 6h, i). Topography, amplitude, and three-dimensional image (1 × 1 μm areas) corroborated the following features: somewhat folded non cutinized cellulose layer, evident and dense packed cellulose microfibrils, visible, regular and parallel layers, minute spacing between layers, and

Author's personal copy

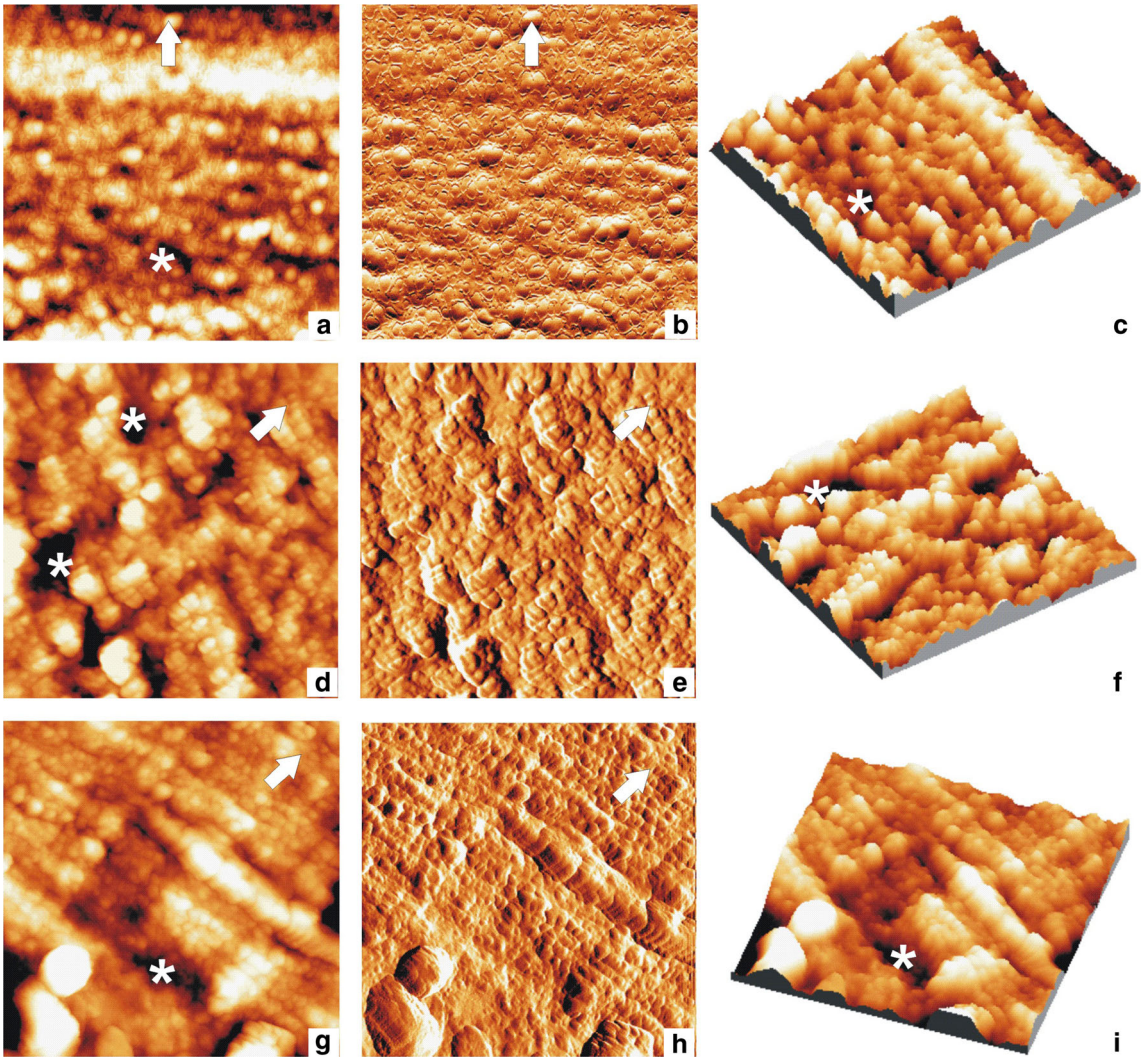


Fig. 7 *Solanum lycopersicum* L. var. cerasiforme AFM micrographs of non cutinized cellulose layer, topography, amplitude, and 3-D image types. **a–c** Raw cherry tomatoes. **d–f** Hydrogen peroxide treated cherry tomatoes. **g–i** Ultrasound cherry tomatoes. *White arrow* indicates outer region of epidermis; *white asterisk* indicates nanopore. Scan sizes, **a–i** is 1 × 1 μm

scarce, irregular, twisted nanopores, randomly distributed, and variables in size (Fig. 7g–i).

Mechanical Properties

Typical force-displacement curves for punctured cherry tomatoes are shown in Fig. 8. Treated and raw fruits presented one fracture peak followed by an abrupt fall in force. The force-displacement pattern resulted similar to those obtained by Petracek and Bukovac (1995), Kabas and Ozmerzi (2008), and Desmet et al. (2003) in cherry tomatoes. Although puncture test takes into account the behavior of the whole fruit (Maury et al. 2009), the skin of cherry tomatoes (treated or untreated) had the major effect on the mechanical properties, contributing more than 90% of the firmness of the fruit before the rupture point, as can be seen in Fig. 8. The minor role of the penetrating force in the flesh (lower than 10% of the

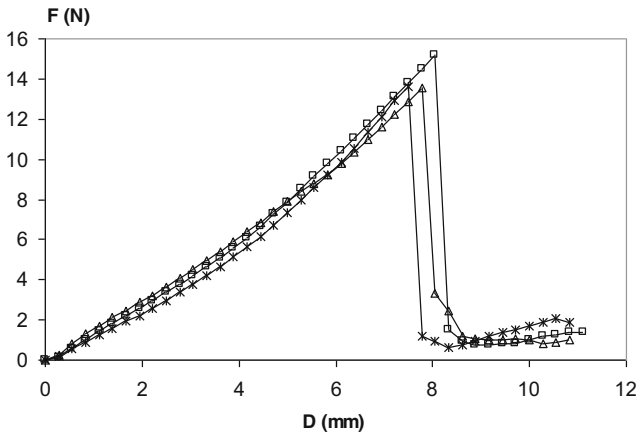


Fig. 8 Typical penetrometric force-displacement curves for raw and treated cherry tomatoes. *Empty square* indicates raw cherry tomatoes; *empty triangle* indicates hydrogen peroxide treated cherry tomatoes; *x mark* indicates ultrasound-treated cherry tomatoes

Author's personal copy

rupture force) had also been reported in unpeeled tomato, cucumber, Japanese pear, and grape (Maury et al. 2009; Sirisomboon et al. 2000; Thompson et al. 1992; Jackman and Stanley 1994).

Mean values of mechanical parameters (rupture force, F_R; deformation at the rupture point, D_R, and mechanical work to break the skin, W) are exhibited in Table 1. MANOVA of treatments was highly significant (treatment $F_{4,\ 156} = 6.\ 96$; $p < 0.0001$). Post-hoc comparisons detected differences between treatment group centroids of raw cherry tomatoes and cherry tomatoes exposed to hydrogen peroxide and ultrasound (Table 1). The first discriminant function derived from DFA accounted for most of the variation (99.6%), and contrasted D_R positively and F_R negatively. DFA only correctly classified the treatments of 59% ($n = 81$) of the random cherry tomatoes test data. Coincidently with MANOVA results, not any response variable was significant to discriminate and consequently to generate clusters of treatments (hydrogen peroxide and ultrasound). Raw cherry tomatoes and ultrasound were better classified (67% correctly classified) than hydrogen peroxide (47% correctly classified) treatments.

Color

The average values of colorimetric L^*, a^*, and b^* parameters and C and h color functions of cherry tomatoes subjected to the different treatments are presented in Table 2. Although the differences in the values for treated and untreated cherry tomatoes were small, the one-way MANOVA of treatments was highly significant for color measurements ($F_{10,\ 40} = 2,\ 95$; $p = 0.0073$). Treatment group centroids were statistically different as the result of post-hoc multiple comparisons (Hotelling tests $p \leq 0.05$), although multivariate means of both raw cherry tomatoes and hydrogen peroxide treatment did not differ statistically (Table 2).

Ultrasound treatment resulted in a decrease in a^*, b^*, and C and in a slight increase in L^* and h mean values. The first discriminant function resulted from DFA explained most of the between-groups (raw and hydrogen peroxide and ultrasound treatment) variance (91.4%), whereas the second discriminant function explained the little variation remaining (8.6%). The discriminating selective variables which contributed most to the first discriminant function among treatments were hue angle (h), chromaticity on a red to green axis (a^*), and blue to yellow axis (b^*). Chromaticity on a red to green axis and on a yellow to blue axis (a^* and b^*) and chroma (C) were the most significant discriminating selective variables for the second discriminant function. The 69% ($n = 26$) of random cherry tomatoes were successfully classified by treatments from DFA. The percentage of successful prediction was 78 and 72% for sonicated and raw fruits, respectively, followed by hydrogen peroxide exposed fruits (60% correctly classified).

Table 1 Mean value ± SD (standard deviation) of F_R, D_R, and W parameters for raw and treated cherry tomatoes

Treatment	F_R (N) ± SD	D_R (mm) ± SD	W (mJ) ± SD	
Raw tomatoes	14.8 ± 1.5	7.6 ± 0.7	48.7 ± 8.1	A
Hydrogen peroxide	14.1 ± 2.1	7.7 ± 0.7	48.3 ± 10.3	B
Ultrasound	13.8 ± 1.6	8.0 ± 0.6	44.4 ± 8.1	B

Post-hoc multiple comparisons using Hotelling tests based on Bonferroni correction $\alpha = 0.05$

Different letters indicate significant differences at $p \leq 0.05$

Relationship Between Structure and Mechanical and Color Parameters

Preserving the structure is a major objective of the postharvest processing of fruits, as changes in structure lead to detrimental changes in texture, flavor, appearance, and mechanical and nutritional properties (Aguilera and Stanley 1999; Sila et al. 2008). The relationship between some materials' properties, in particular transport and rheological ones, and microscopic features of plant tissues is well known. In general, at the cellular and tissue levels, the three major structural factors that contribute to mechanical behavior of plant-based foods are turgor pressure within individual cells (i.e., the force exerted on the cell membrane by intracellular fluid), the cell wall rigidity, and the cell-cell adhesion, determined by the integrity of the middle lamella and the plasmodesmata (Jackman and Stanley 1995; Waldron et al. 2003; Alzamora et al. 2000, 2008). In the epidermis, composition and architecture also affect the mechanical behavior of the epidermal cell walls (Domínguez et al. 2011; Lara et al. 2014).

As seen in Fig. 8, fruit skin played the most important role in the overall firmness and force-deformation pattern is more linked to the skin rheological characteristics. Accordingly, alterations in skin architecture would be undoubtedly important on puncture response of treated cherry tomatoes. In relation to crack-resistance, Cotner et al. (1969) reported cracks associated to epidermal cells morphology and mesocarp vascular pattern. Matas et al. (2004) analyzed fruit tensile properties and structure of Inbred 10 and Sweet 100 cherry tomatoes, which differ in susceptibility to cracking. Authors proposed that CM served as a "tensile skin" whose mechanical properties and behavior were hardly correlated with thickness. Bargel and Neinhuis (2005) studied the structure and mechanical properties (elasticity, strength, and failure strain) of fruit skin in three tomato cultivars at different ripening stages. They concluded that during ripening, the decrease of cuticle extensibility had implications concerning to cracking susceptibility, harvesting, transportation, and extended storage. Chaib et al. (2007) investigated the texture at the

Author's personal copy

Table 2 Mean value ± SD (standard deviation) of L^*, a^*, and b^* parameters, and C and h functions for raw and treated cherry tomatoes

Treatment	L^* ± SD	a^* ± SD	b^* ± SD	C ± SD	h ± SD	
Raw	31.5 ± 2.1	31.9 ± 2.7	39.3 ± 3.8	50.7 ± 4.4	50.9 ± 1.8	A
Hydrogen peroxide	31.8 ± 1.5	32.1 ± 1.8	39.9 ± 2.2	51.2 ± 2.6	51.2 ± 1.3	A
Ultrasound	32.3 ± 1.5	28.6 ± 1.9	37.3 ± 2.3	47.1 ± 2.6	52.5 ± 1.6	B

Post-hoc multiple comparisons using Hotelling tests based on Bonferroni correction $\alpha = 0.05$

Different letters indicate significant differences at $p \leq 0.05$

rheological, sensory, morphological, and genetic levels of cherry tomatoes, and established correlations between some texture traits and parameters of the epicarp cellular structure.

It has also been reported that isolated CM of cherry tomato fruit exhibited a high elastic modulus but a low work of fracture, while epidermal and subepidermal tissues are capable of significant elastic deformation before rupture. Thus, the CM can be interpreted as a membrane that stiffens the cell walls while epidermal and subepidermal cells give strength to the CM (Domínguez et al. 2011). Epidermal and subepidermal tissues would behave as energy sinks that absorbs strain energy: as the cuticle and cutinized layer deform such more energy is needed to propagate a crack through cell walls than through isolated CM. Accordingly, CM, epidermal, and subepidermal cells have a significant role in supporting mechanical stress. Both treatments provoked small changes in CM and epidermal and subepidermal tissues. As seen en LM, after hydrogen peroxide treatment, cherry tomatoes appeared similar to the raw fruit but ultrasound treatment caused notorious swelling of walls and incipient plasmolysis (with consequent loss of turgor) of subepidermal cells. This effect was very notorious in mesocarp but this tissue has a minor contribution to mechanical properties. Changes analyzed with TEM confirmed that both treatments altered the non cutinized cellulose layer and slightly accentuated the non cutinized cellulose layer and the cuticular membrane transition. After hydrogen peroxide exposure, a looser cellulose microfibrils framework was observed, while ultrasound-treated fruits showed an evident and dense packed framework of cellulose microfibrils. AFM structure study showed that hydrogen peroxide and ultrasound treatments affected the nanostructure of outer tangential epidermal cell wall, generating changes in the cellulose domain, loosing or compressing the cellulose layer, respectively, and altering the cellulose aggregates and nanofracture morphology. While ultrasound generated well-delimited transitions between cuticle, cutinized cellulose layer, and non cutinized cellulose layer, hydrogen peroxide treatment maintained the gradual transition between them. The nanoporosity observed in the non cutinized cellulose layer of hydrogen peroxide treated fruit would confirm the findings reported by Miller (1986). This author mentioned the oxidation of cell wall polysaccharides by hydrogen peroxide treatment as a potential mechanism for cell wall breakdown in plants.

There were small but significant differences in the mechanical behavior between treated and raw fruits. Although ultrasound and hydrogen peroxide exposure induced different structure changes, mechanical parameters did not allow discriminating between treatments. In sonicated fruits, the decline in F_R and the increase in D_R would be mainly associated with the loss of turgor pressure due to plasmolysis of subepidermal cells, while the slight epicarp compression (dense packed cellulose microfibrils, scarce nanopores) would not be enough to counteract these adverse changes. In cherry tomato fruits treated with hydrogen peroxide, the loosing of cellulose microfibrils network in the cutinized cellulose layers and the formation of cellulose aggregates and nanopores in the cellulose layer would be the responsible of the small decrease in F_R.

Color study revealed small but significant differences in colorimetric parameters and functions among ultrasound treated and raw fruits. As indicated by microscopic observations, both treatments assayed altered the epicuticular wax layer but this modification was more severe in fruits exposed to ultrasound, which exhibited the major differences in L^*, a^*, and hue values as compared to raw fruit. Thus, this change in wax coverage would alter light reflection and would traduce in sonicated fruits slightly lighter and more orange than the control. These results would be in agreement with those reported in *Vitis labrusca* L. (grape berry) fruits treated by hydrogen peroxide and ultrasound (Fava et al. 2011). Epicuticular wax structural modification was very severe in ultrasound-treated grapes, which exhibited the major differences in L^* regarding the raw fruit. However, changes in epicuticular waxes of fruits undergone peroxide hydrogen and UV-C radiation were not so different to support significant differences between both treatments.

Conclusions

Epicuticular wax layer alteration, accentuated transition between cellulose layer and cuticular membrane of the outer tangential epidermal cell wall, aggregation of cellulose microfibrils with peculiar pattern organization and nanofractures, variables in shape and size, contraction of epicarp, plasmolysis of subepidermal and mesocarp cells, and swelling of walls

Author's personal copy

were some of the main structure features corroborated after hydrogen peroxide and/or ultrasound treatments. The color of sonicated fruits was slightly affected due to the disruption of the wax layer; the fruits became brighter and more orange. Exposure to ultrasound or to hydrogen peroxide slightly affected puncture parameters F_R, D_R, and W but there were not significant differences between the mechanical behavior of treated fruits. The mechanical response could be partially explained by the alterations in the micro, ultra, and nanostructure of the tissues.

The low impact on mechanical and color properties would support the application of these emerging techniques, at the dose assayed, for cherry tomatoes decontamination in terms of these quality attributes.

Acknowledgements The authors acknowledge the valuable AFM technical assistance of Silvio Ludueña from CMA-FCEyN-UBA, and the financial support from University of Buenos Aires, CONICET, and ANPCyT of Argentina and from BID.

References

Aguilera, J. M., & Stanley, D. W. (1999). *Microstructural principles of food processing and engineering. 2nd Ed (chapter 6)*. Gaithersburg: An Aspen Publication.

Allende, A., Tomás-Barberán, F. A., & Gil, M. I. (2006). Minimal processing for healthy traditional foods. *Trends in Food Science and Technology, 17*, 513–519.

Alzamora, S. M., Castro, M. A., Nieto, A. B., Vidales, S. L., & Salvatori, D. M. (2000). The role of tissue microstructure in the textural characteristics of minimally processed fruits. In S. M. Alzamora, M. S. Tapia, & A. López-Malo (Eds.), *Minimally processed fruits and vegetables* (pp. 153–171). Gaithersburg: Aspen Publishers Inc..

Alzamora, S. M., Viollaz, P. E., Martínez, V. Y., Nieto, A. B., & Salvatori, D. M. (2008). Exploring the linear viscoelastic properties structure relationship in processed fruit tissues. In G. E. Gutiérrez-López, G. V. Barbosa-Cánovas, J. Welti-Chanes, & E. Parada-Arias (Eds.), *Food engineering: integrated approaches* (pp. 133–214). New York: Springer.

Baker, E. A. (1982). Chemistry and morphology of plant epicuticular waxes. In D. F. Cutler, K. L. Alvin, & C. E. Price (Eds.), The plant cuticle, Vol. 10 (pp. 139–165). Linnean Society Symposium Series. London: Academic Press.

Balasundram, N., Sundram, K., & Samman, S. (2006). Phenolic compounds in plants and agro-industrial by-products: antioxidant activity, occurrence, and potential uses. *Food Chemistry, 99*, 191–203.

Bargel, H., & Neinhuis, C. (2005). Tomato (*Lycopersicon esculentum* Mill.) fruit growth and ripening as related to the biomechanical properties of fruit skin and isolated cuticle. *Journal of Experimental Botany, 56*, 1049–1060.

Carpita, N. C., & Gibeaut, D. M. (1993). Structural models of primary cell walls in flowering plants: consistency of molecular structure with the physical properties of the walls during growth. *Plant Journal, 3*, 1–30.

Chaib, J., Devaux, M. F., Grotte, M. G., Robini, K., Causse, M., Lahaye, M., et al. (2007). Physiological relationship among physical, sensory, and morphological attributes of texture in tomato fruits. *Journal of Experimental Botany, 8*, 1915–1925.

Cosgrove, D. J. (2001). Wall structure and wall loosening. A look backwards and forwards. *Plant Physiology, 125*, 131–134.

Cotner, S. D., Burns, E. E., & Leeper, P. W. (1969). Pericarp anatomy of crack-resistant and susceptible tomato fruits. *Journal of American Society of Horticultural Science, 94*, 136–137.

Desmet, M., Lammertyn, J., Scheerlinck, N., Verlinden, B. E., & Nicolai, B. M. (2003). Determination of puncture injury susceptibility of tomatoes. *Postharvest Biology and Technology, 27*, 293–303.

Domínguez, D., Cuartero, J., & Heredia, A. (2011). An overview on plant cuticle biomechanics. *Plant Science, 181*, 77–84.

Esau, K. (1977). *Anatomy of seed plants* (2nd ed.). New York: Wiley.

Fava, J., Hodara, K., Nieto, A. B., Guerrero, S. N., Alzamora, S. M., & Castro, M. A. (2011). Structure (micro, ultra, nano), colour and mechanical properties *of Vitis labrusca* L. (grape berry) fruits treated by hydrogen peroxide, UV-C irradiation and ultrasound. *Food Research International, 44*, 2938–2948.

George, B., Kaur, C., Khurdiya, D. S., & Kapoor, H. C. (2004). Antioxidants in tomato (*Lycopersium esculentum*) as a function of genotype. *Food Chemistry, 84*, 45–51.

Guerrero, S. N., López-Malo, A., & Alzamora, S. M. (2001). Effect of ultrasound on the survival of *Saccharomyces cerevisiae.* Influence of temperature, pH and amplitude. *Innovative Food Science and Emerging Technologies, 2*, 31–39.

Holloway, P. J. (1982). The chemical constitution of plant cutins. In D. F. Cutler, K. L. Alvin, & C. E. Price (Eds.), The plant cuticle, Vol. 10 (pp. 45–85). Linnean Society Symposium Series. London: Academic Press.

Jackman, R. L., & Stanley, D. W. (1994). Influence of the skin on puncture properties of chilled and nonchilled tomato fruit. *Journal of Texture Studies, 25*, 221–230.

Jackman, R., & Stanley, D. (1995). Perspectives in the textural evaluation of plant foods. *Trends in Food Science and Technology, 6*, 187–194.

Jeffree, C. E., Baker, E. A., & Holloway, P. J. (1976). Origins of the fine structure of plant epicuticular waxes. In C. H. Dickinson & T. F. Preece (Eds.), *Microbiology of aerial plant surface* (pp. 119–158). London: Academic Press.

Juven, B. J., & Pierson, M. D. (1996). Antibacterial effects of hydrogen peroxide and methods for its detection and quantitation. *Journal of Food Protection, 59*, 1233–1241.

Kabas, O., & Ozmerzi, A. (2008). Determining the mechanical properties of cherry tomato varieties for handling. *Journal of Texture Studies, 39*, 199–209.

Lara, I., Belge, B., & Goulao, L. F. (2014). The fruit cuticle as a modulator of postharvest quality. *Postharvest Biology and Technology, 87*, 103–112.

López-Malo, A., Guerrero, S., & Alzamora, S. M. (1999). *Saccharomyces cerevisiae* thermal inactivation kinetics combined with ultrasound. *Journal of Food Protection, 62*, 1215–1217.

Martínez-Valverde, I., Periago, M. J., Provan, G., & Chesson, A. (2002). Phenolic compounds, lycopene and antioxidant activity in commercial varieties of tomato (*Lycopersicon esculentum*). *Journal of the Science of Food and Agriculture, 82*, 323–330.

Mason, T. J. (1990). *Sonochemistry: the uses of ultrasound in chemistry*. Cambridge: Royal Society of Chemistry.

Matas, A. J., Cobb, E. D., Bartsch, J. A., Paolillo, D. J., & Niklas, K. J. (2004). Biomechanics and anatomy of *Lycopersicum esculentum* fruit peels and enzyme-treated samples. *American Journal of Botany, 91*, 352–360.

Maury, C., Madieta, E., Le Moigne, M., Mehinagic, E., Siret, R., & Jourjon, F. (2009). Development of a mechanical texture test to evaluate the ripening process of cabernet franc grapes. *Journal of Texture Studies, 40*, 511–535.

McGarigal, K., Cushman, S., & Stafford, S. (2000). *Multivariate statistics for wildlife and ecology research*. New York: Springer-Verlag.

Miller, R. A. (1986). Oxidation of cell wall polysaccharides by hydrogen peroxide: a potential mechanism for cell wall breakdown in plants. *Biochemical and Biophysical Research Communications, 141*, 238–244.

Author's personal copy

Pagliarini, E., Monteleone, E., & Ratti, S. (2001). Sensory profile of eight tomato cultivars (*Lycopersicon esculentum*) and its relationship to consumer preference. *Italian Journal of Food Science, 13*, 285–296.

Petracek, P. D., & Bukovac, M. J. (1995). Rheological properties of enzymatically isolated tomato fruit cuticle. *Plant Physiology, 109*, 675–679.

Pinelo, M., Arnous, A., & Meyer, A. S. (2006). Upgrading of grape skins: significance of plant cell-wall structural components and extraction techniques for phenol release. *Trends in Food Science and Technology, 17*, 579–590.

Quinn, G. P., & Keough, M. J. (2002). *Experimental design and data analysis for biologists*. New York: Cambridge University Press.

Raffellini, S., Schenk, M., Guerrero, S. N., & Alzamora, S. M. (2011). Kinetics of *Escherichia coli* inactivation employing hydrogen peroxide at varying temperatures, pH and concentrations. *Food Control, 22*, 920–932.

Rao, A. V., & Agarwal, S. (2000). Role of antioxidant lycopene in cancer and heart disease. *Journal of the American College of Nutrition, 19*, 563–569.

Reynolds, E. S. (1963). The use of lead citrate at high pH as an electron opaque stain in electron microscopy. *Journal of Cell Biology, 17*, 208–212.

Sao José, J. F. B., & Vanetti, M. C. D. (2012). Effect of ultrasound and commercial sanitizers in removing natural contaminants and *Salmonella enterica* Typhimurium on cherry tomatoes. *Food Control, 24*, 95–99.

Sharoni, Y., & Levi, Y. (2006). Cancer prevention by dietary tomato lycopene and its molecular mechanisms. In A. V. Rao (Ed.), *Tomatoes, lycopene & human health* (pp. 111–125). Barcelona: Caledonian Science Press Ltd..

Sila, D. N., Duvetter, T., De Roeck, A., Verlent, I., Smout, C., Moates, G. K., et al. (2008). Texture changes of processed fruits and vegetables: potential use of high-pressure processing. *Trends in Food Science and Technology, 19*, 309–319.

Sirisomboon, P., Tanaka, M., Akinaga, T., & Kojima, T. (2000). Evaluation of the texture properties of Japanese pear. *Journal of Texture Studies, 31*, 665–677.

Spurr, A. R. (1969). Low-viscosity epoxy resin embedding medium for electron microscopy. *Journal of Ultrastructure Research, 26*, 31–43.

Thompson, R. L., Fleming, H. P., & Hamann, D. D. (1992). Delineation of puncture forces for exocarp and mesocarp tissues in cucumber fruit. *Journal of Texture Studies, 23*, 169–184.

Waldron, K. W., Parker, M. L., & Smith, A. C. (2003). Plant cell walls and food quality. *Comprehensive Reviews in Food Science and Food Safety, 4*, 101–119.

Wang, W., Ma, X., Zou, M., Jiang, P., Hu, W., Li, J., et al. (2015). Effects of ultrasound on spoilage microorganisms, quality, and antioxidant capacity of postharvest cherry tomatoes. *Journal of Food Science, 80*, C2117–C2126.

Wattendorff, J., & Holloway, P. J. (1980). Studies on the ultrastructure and histochemistry of plant cuticles: the cuticular membrane of *Agave americana* L. *in situ*. *Annals of Botany, 46*, 13–28.

Wilcox, J. K., Catignani, G. L., & Lazarus, S. (2003). Tomatoes and cardiovascular health. *Critical Reviews in Food Science and Nutrition, 43*, 1–18.